Investigation of the interactions between methylene blue and intramolecular G-quadruplexes: an explicit distinction in electrochemical behavior

Ting Cao,[a] Fang-Ting Zhang,[a] Liang-Yuan Cai,[a] Ying-Lin Zhou,[a]* Niklaas J. Buurma,[b]* and Xin-Xiang Zhang[a]*

G-quadruplex sequences exist in eukaryotic organisms and prokaryotes, and the investigation of interactions between G-quadruplexes and small molecule ligands is important for gene therapy, biosensor fabrication, fluorescence imaging and so on. Here, we investigated the behaviour of methylene blue (MB), an electroactive molecule, in the presence of different intramolecular G-quadruplexes by electrochemical method using a miniaturized electrochemical device based on its intrinsic electrochemical property. Although the effects of MB on different intramolecular G-quadruplex structures are not obvious by circular dichroism spectroscopy, distinct differences in binding affinities of MB with different intramolecular G-quadruplexes were fast and easily observed by the electrochemical technique. At the same time, for the human telomerase G-rich sequence (HT), the diffusion current of MB changed sensitively under different ion conditions due to the formation of different conformations of HT, which indicated that our electrochemical method has the potential to study the influence of metal ions on the conformations of the G-quadruplexes with simplicity, rapid response and low cost. From all these, new stacking mechanism and rule were obtained, which were also validated by docking studies and isothermal titration calorimetry (ITC).

Introduction

Guanine-rich nucleic acid sequences have the ability to self-assemble into DNA structures comprising of several planar molecular squares, denoted as G-tetrads, or G-quartets.[1] In each G-quartet, four guanine bases mutually interact through Hoogsteen hydrogen bonds clockwise or anticlockwise (from hydrogen bond donor to acceptor) in a cyclic arrangement. Consecutive stacking of two or more G-quartets gives rise to four-stranded helical structures called G-quadruplexes.[2] In general, the polymorphisms of G-quadruplexes include different strand orientations (parallel, antiparallel and mixed hybrid type), molecularities (tetramolecular, bimolecular and unimolecular), glyosidic conformations (syn-form and anti-form) and topologies (lateral, diagonal, V-shaped and double chain reversal loops).[3] The structures of G-quadruplex are further complicated not only due to different loop types linking G-rich units and the relative orientation of the G-rich sequence units but also higher-order architecture and bulges in G-quadruplexes and so on, which have broadened the definition of G-quadruplex.[4]

G-quadruplex sequences are believed to exist widely in the genome, and play an important role in biological processes, such as recombination, transcription, replication and translation.[5] They also exist in chromosome telomeres and the proximal promoter regions of human oncogenes.[6, 7] Up to now, more than 70, 000 sequences in the genome have been identified as sequences that have the potential to form quadruplex conformations.[8] The formation and stabilization of quadruplex structure can influence the biological functions of quadruplex sequences to some extent, such as gene expression. Therefore, the discoveries of ligands which facilitate and stabilize quadruplex folding has become a research direction for chemotherapy of cancer.[9] Usually, quadruplexes can be stabilized by alkali metal ion and other cations, such as K^+, Na^+ and NH_4^+ and so on.[3] There also exist aromatic ligands which can bind and stabilize quadruplex effectively by π-π stacking interactions.[9, 10] For example, quarfloxin, a fluoroquinolone derivative, is a successful candidate drug entering human clinical trials for cancer therapy.[11] In addition to the applications in oncology, quadruplex ligands are also implemented in the field of biosensors, fluorescence imaging and even assembly of nanostructures.[12-14] Therefore, the study of quadruplex ligands has been gaining in importance.

Electrochemical method, a simple and fast technique, has been used as a good tool to study G-quadruplexes and screen of G-quadruplex ligands.[15,16] Methylene blue (MB), a kind of phenothiazine, is positively charged in solution and is used as a common electrochemical indicator in DNA based biosensors.[17] It has been reported that MB has a favored binding with the guanine-rich sequence and this may contribute to the formation of tetramolecular G-quadruplex.[18] MB can also act as a G-quadruplex binding probe because of its stronger binding with G-quadruplex over DNA double strands.[13] Until now, the interaction studies of MB and G-quadruplexes are mainly focused on a limited number of specific G-quadruplex-forming sequences and the studies of G-quadruplexes interaction with small molecules were usually carried out by nuclear magnetic resonance (NMR), mass spectroscopy (MS) and X-ray diffraction that require expensive equipment and considerable experimental time.[19-21]

Here, we made use of the intrinsic electrochemical property of MB to systematically explore its binding mechanisms with a series of common intramolecular G-quadruplex sequences by electrochemical method, which has distinct advantages of simplicity, miniaturization, rapid response, low cost and that only 20 μL solution was required for the experiments presented here. Compared with other works,[13, 22, 23] we used electrochemical method to distinguish the difference for binding affinities of MB with different intramolecular G-quadruplexes, which greatly enriched the study range of G-quadruplexes. From the electrochemical results, we infer that the ability of MB interacting with intramolecular G-quadruplexes depends on conformations and sequence characteristics. The human telomerase G-rich sequence (HT)

[a] *Beijing National Laboratory for Molecular Sciences (BNLMS), MOE Key Laboratory of Bioorganic Chemistry and Molecular Engineering, College of Chemistry, Peking University. No.202 Chengfu Road, Haidian District, Beijing 100871, China. E-mail: zhouyl@pku.edu.cn, zxx@pku.edu.cn.*

[b] *Physical Organic Chemistry Centre, School of Chemistry, Cardiff University. Main Building, Park Place, Cardiff, CF10 3AT (UK). E-mail: buurma@cardiff.ac.uk.*

† Footnotes relating to the title and/or authors should appear here.

Electronic Supplementary Information (ESI) available: [details of any supplementary information available should be included here]. See DOI: 10.1039/x0xx00000x

was selected to confirm this conformation dependence and indeed showed explicit difference on the diffusion current of MB under different ion conditions in few seconds. Our results are not consistent with the previous assumption that the binding site of MB with G-quadruplex is the same as that of hemin, a porphyrin molecule, with G-quadruplex. Hemin shows a more obvious ability to distinguish G-quadruplexes with different conformations[13, 24] We therefore propose that MB possibly stacks with intramolecular G-quadruplexes by interacting with up to two guanines because of its molecular size, which is different with intermolecular G-quadruplexes.[23] These results were validated by circular dichroism (CD), molecular docking and isothermal titration calorimetry (ITC). Thermodynamic parameters for MB interacting with intramolecular quadruplexes possessing different conformations were also further demonstrated and characterized.

Experimental

Reagents and Apparatus

All DNA oligonucleotides used in this experiment (Table S1) were synthesized by Sangon Biological Engineering Technology & Services Co., Ltd. (Shanghai, China) and purified by HPLC. The DNA concentrations were calibrated at 260 nm by Thermo Scientific Nanodrop 2000 Spectrophotometer (MA, USA). Potassium chloride and sodium chloride were ultrapure grade and bought from Alfa Aesar (MA, USA). MB and HCl (MOS pure) were purchased from Beijing Chemical Reagent Co. (Beijing, China). Tris-base was of ultrapure grade and obtained from CalbioChem (Darmstadt, Germany). All reagents were stored at room temperature and the water used throughout was obtained from a Milli-Q purification system (Bedford, MA, USA). A CHI 660C electrochemical workstation from Chenhua Instruments Co. (Shanghai, China) was employed to carry out the electrochemical experiments.

CD study

CD spectra (220-350 nm) were recorded on a JASCO J-815 CD spectrometer (Japan) in a quartz cell of 1 mm optical path length at room temperature. G-quadruplex DNA solutions (20 μM) were prepared in working buffer (25 mM Tris-HCl, pH 7.4, containing 100 mM KCl). To explore whether MB has an influence on the structural stability of the G-Quadruplex, excess MB (200 μM) was added into the DNA solutions to guarantee a complete interaction. Scanning speed was 100 nm/min, bandwidth was 2.0 nm and data interval was 0.1 nm. The CD spectra were averaged from three scans.

Electrochemical Measurements

All the electrochemical measurements were conducted in a miniaturized device (Figure S1) described in our previous work.[25] A carbon fiber ultramicroelectrode (CFUE) was fabricated similarly to our previous procedure.[25] The CFUE was inserted into a micropipet tip containing a 20 μL analyte solution, and used as the working electrode. Together with an Ag/AgCl reference electrode and a platinum counter electrode, the CFUE constituted a three-electrode system. Square wave voltammetry (SWV) was recorded with a potential range from -0.6 V to 0.2 V, an incremental potential of 4 mV, a pulse amplitude of 25 mV and a frequency of 200 Hz. Cyclic voltammetry (CV) was recorded with a potential range between -0.6 V and 0.1 V and a sampling interval of 5 mV.

Docking Studies

Docking molecular simulation was performed in Autodock Vina 1.1.2 modelling.[26] The human telomere (HT) G-quadruplex structures (PBD 1KF1, 2E4I and 143D) were selected according to the sequence length and conformation in the nucleic acid database.[27-29] Usually, we chose the first model as a target for the next docking process if multiple models existed. The files were pretreated with removing ligands, metal ion and/or water molecules by UCSF Chimera, which was also used to visualize the output PDBQT files after molecular docking with its ViewDock extension.[30] The grid dimensions were 40Å×40Å×50Å, 40Å×40Å×40Å and 40Å×40Å×40Å, which encompassed both the corresponding G-quadruplexes and some other additional space.

ITC

The titrations of MB to G-quadruplex DNAs in working buffer were performed on MicroCal iTC 200 (GE Healthcare, USA) at 25°C. Stirring speed of the cell contents was 1000 rpm and a reference power of 3 μCal/sec was applied in the instrument. 50 μM nucleic acids were placed in the sample cell with a 280 μL sample volume, into which a 500 μM MB solution was added stepwise. The reference cell was filled with ultrapure water. The titrations were performed automatically every 150 seconds, and 20 injections were accomplished in total. Each injection lasted for 4 seconds with a 2 μL ligand solution. Dilution experiments were conducted by adding MB into working buffer under the same experimental conditions. The raw data were processed by Origin and the integrated heat data were analyzed by ITC data-fitting software IC-ITC.[31] All the sample solutions were filtered through 0.22 μm filter before titrations.

Results and discussion

The CD spectra of different intramolecular G-quadruplex structures in the presence of MB

Many G-rich sequences tend to form G-quadruplex structures in the presence of K^+ or Na^+ and show a characteristic CD signal.[3] The characteristic CD signal is produced by the asymmetrical conformation when G-quartets stack on each other. For G-quadruplexes with parallel conformation, the CD spectra exhibit a negative band at 240 nm and a positive band at 260 nm. The CD spectra of antiparallel G-quadruplexes have a negative band at 260 nm and positive bands at both 240 nm and 295 nm. Positive bands at both 260 nm and 295 nm and negative band at 240 nm in one CD spectrum indicate a coexisting or mixed hybrid structure.[3] Different conformation characteristics of G-quadruplexes are shown in Figure S2. For a random sequence without secondary structure, the CD spectrum only shows a positive peak at 280 nm and a negative peak at 250 nm, which

results from the two characteristic π-π transitions in guanine absorption. In the following, several common intramolecular G-quadruplex DNA sequences (The information about the sequences is shown in Table S1) were involved in the study of the interaction between G-quadruplexes and MB. The CD spectra of the G-rich nucleic acids in working buffer confirm the conformations of common G-quadruplex structures (Table S2). The CD spectra for the G-quadruplexes in the presence of MB were also included. MB itself had no CD signals between 220-350 nm (Figure S3).

As shown in Table S2, CD spectroscopy is a convenient and effective tool to investigate the conformations of G-quadruplexes and can realize a clear characterization of different G-quadruplexes. Excess MB can cause a positive, negative or negligible influence on the configurations of different intramolecular G-quadruplexes. Among these, the coexisting or mixed hybrid type shows relatively clear and opposite phenomena, in which MB stabilizes parallel proportion for HT (240 nm and 260 nm) while it stabilizes antiparallel proportion for Bcl-2 (295 nm). However, these effects of MB on different intramolecular G-quadruplex structures are not distinct, even though 10-fold excess of MB are added. Thus, it is impossible to reach an exact conclusion that the existence of MB has a noteworthy impact on the conformation of G-quadruplexes. Also, it was difficult to determine the binding strength simply from CD spectra. Thus, considering the intrinsic electrochemical property of MB, the electrochemical behavior of MB in the presence of different G-quadruplexes was investigated to establish the order of binding affinities and to further illuminate the interactions between G-quadruplexes and MB.

Electrochemical assay for the interactions between MB and different intramolecular G-quadruplexes

The diffusion currents of 10 μM MB in working buffer were measured by SWV in the absence and presence of 10 μM of different G-quadruplexes in our designed miniaturized electrochemical device (Figure S1). The results are shown in Figure 1 and Table S3. The diffusion currents of MB before and after several consecutive SWV measurements are recorded in Figure S4 to ensure that nonspecific adsorption of DNA on the microelectrode can be ignored.

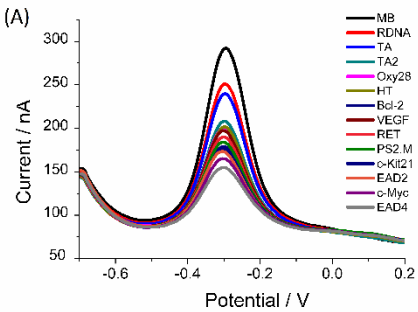

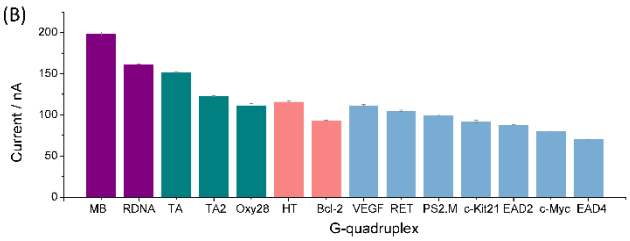

Figure 1. (A) SWVs of MB in the presence of 10 μM of different G-quadruplexes, and (B) their corresponding SWV peak currents (the bars in green represent antiparallel G-quadruplexes, the bars in brick-red represent coexisting or mixed hybrid G-quadruplexes and the bars in light blue represent parallel G-quadruplexes).

Although MB did not change the conformations of intramolecular G-quadruplexes according to CD, clear discrimination of diffusion current could be obtained in the SWV assays of MB in the presence of different intramolecular G-quadruplexes as shown in Figure 1A. The typical SWV potential of MB in the absence and presence of different G-quadruplexes shows a slight shift, but the currents of MB are changing sharply with equivalent different intramolecular G-quadruplexes. We attribute the lower currents to stronger binding.[32] The data thus shows that different G-quadruplexes present different binding abilities with MB, mainly depending on the intrinsic structure characteristics of the G-rich nucleic acids. Remarkably, there exists a relatively apparent distinction between parallel and antiparallel G-quadruplexes. From Figure 1B, intramolecular parallel G-quadruplexes (light blue) interact with MB more tightly than antiparallel G-quadruplexes (green). The mixed hybrid G-quadruplexes (brick-red) are found in both parallel G-quadruplexes region (Bcl-2) and antiparallel G-quadruplexes region (HT). This is in harmony with the CD result that Bcl-2 has a stronger absorption at 260 nm (characteristic absorption band of parallel conformation) while HT has a stronger absorption at 295 nm (characteristic absorption band of antiparallel conformation). Parallel G-quadruplexes tend to have a smaller steric hindrance than antiparallel G-quadruplexes because of the open side of the terminal G-quartet plane, which suggests a terminal stacking mechanism might exist between parallel G-quadruplex and MB. This agrees with the prediction in our previous work.[13] The mixed hybrid G-quadruplexes fall into the antiparallel and parallel regions, and the gap between parallel conformation zone and antiparallel conformation zone was not large. This phenomenon is not consistent with the terminal interaction rule observed from the interaction between G-quadruplexes and hemin completely, which can bind with G-tetrad plane of four guanines in G-quadruplex via end stacking. Also, in the interaction of hemin and G-quadruplexes, the interactional strength with intramolecular parallel G-quadruplexes is much larger than that with antiparallel G-quadruplexes.[24] A similarly large difference in affinities is not observed here. A possible explanation may be that MB gives a

weaker interaction with intramolecular G-quadruplexes than hemin, which has a large π-aromatic surface and can stack on terminal G-tetrad plane fully. This can also be illustrated by CD spectra in Table S2, in which MB does not exhibit a significant influence on different conformations of G-quadruplexes.

Studies of HT sequence by SWV and docking

In order to further estimate the influence of G-quadruplex conformations on binding affinity to MB, the interaction of MB with a single G-quadruplex sequence, HT, which forms different quadruplex topologies under different ionic conditions, was explored under different ion conditions. HT, the human telomerase G-rich sequence, presented as coexisting or mixed hybrid type in K^+ ion-rich solution while it converted to an antiparallel type in Na^+ ion-rich solution (Figure 2A). The SWV currents of MB were measured in the presence of HT with K^+ and Na^+ respectively. As shown in Figure 2B, the diffusion current of 10 μM MB in the absence of quadruplex in 25 mM Tris-HCl containing 100 mM KCl or 100 mM NaCl are almost the same. However, different diffusion currents are achieved when HT is added into the two solutions. The antiparallel HT type causes a relatively low influence on diffusion current of MB while the parallel topology of HT causes a bigger change, which is in accordance with the results shown in Figure 1. Here, the change of the electrochemical signal is thus directly related to the conformation of the G-quadruplex, which can be obtained with only 20 μL solution in few seconds by the miniaturized electrochemical device.

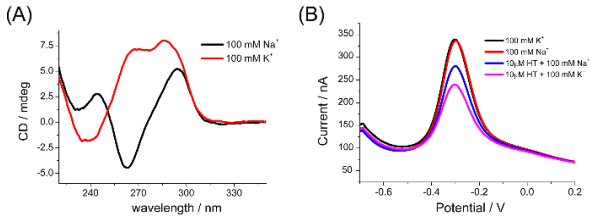

Figure 2. (A) CD spectra of 10 μM HT in different ion conditions; (B) SWVs of MB with HT in different ion conditions. The concentration of MB was 10 μM.

The interaction mechanisms between the HT sequence in different conformations and MB were further analyzed by molecular docking. MB was docked with parallel, antiparallel and mixed hybrid G-quadruplex conformations of HT sequences using Autodock Vina 1.1.2 modeling software, and the results are recorded in Figure 3.

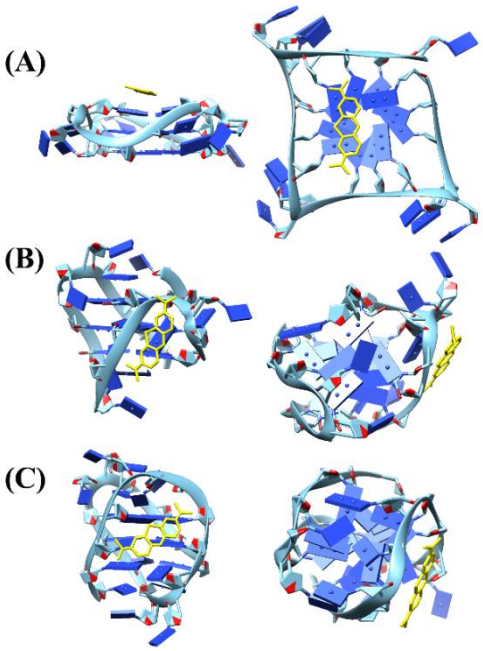

Figure 3. Schematic illustrations of the binding modes between MB and HT G-quadruplexes with (A) parallel, (B) mixed hybrid and (C) antiparallel conformations. Left pictures are side views of the G-quartets, and right ones are top views.

The docking results suggest that MB is smaller than the plane consisting of four guanines in the terminal G-tetrad and that MB is unable to fully cover the terminal G-tetrad plane. In the parallel conformation, G-quadruplex exposes its terminal plane fully and it is more possible to interact with MB through two guanines, which is limited by the molecular size of MB (Figure 3A, binding affinity was -6.1 kcal/mol). In the mixed hybrid conformation, because of steric hindrance of G-quadruplex, MB tends to stack with the adenine base in the backbone (Figure 3B, binding affinity was -5.9 kcal/mol). In the antiparallel conformation, MB only interacts with G-quadruplex by electrostatic interaction with phosphate backbone (Figure 3C, binding affinity was -5.8 kcal/mol). Therefore, we suppose that MB interacts with intramolecular G-quadruplexes by stacking with up to two guanine base planes, which is different from intermolecular G-quadruplexes. Electrostatic (between MB and DNA phosphate backbone) or other interactions (maybe π-π partial vertical overlap between π electron cloud in guanines of G-quartets and π electron cloud in MB) may exist between antiparallel G-quadruplexes and MB, which can be a good proof that some antiparallel G-quadruplexes are slightly stronger than a random DNA sequence interacting with MB in electrochemical results. This assumption is favored by the molecule size of MB, the molecular docking and the CD spectra before and after the addition of MB to G-quadruplex solutions. However, even though the interaction between MB with G-quadruplexes was not obvious in the CD spectra, the electrochemical method based on the intrinsic electroactivity of MB provided credible binding information.

Binding discrimination studies of MB with G-quadruplex sequence and RDNA by CV

Different G-quadruplex sequences bound with MB to a different extent. In addition, there existed a clear discrimination of binding strength between binding to G-quadruplexes and to a random sequence RDNA with the same sequence length (Figure 1 and Table S3). We chose a G-quadruplex sequence, EAD2, as a G-quadruplex model to investigate the discrimination of electrochemical behavior of MB in the presence of G-quadruplex and RDNA. From Figure S5, EAD2 and RDNA at the same concentration decrease the diffusion current of MB to a different degree. Typical CV behavior of 5 μM MB in the absence and presence of DNA with different R value (R is the concentration ratio of DNA to MB) is shown in Figure 4 and Table S4.

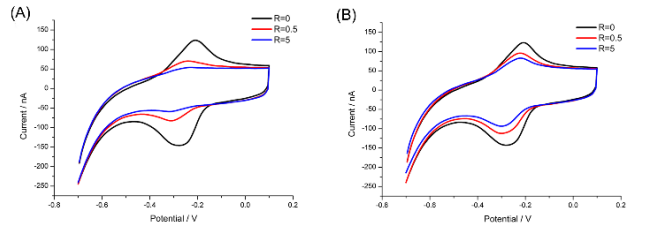

Figure 4. Cyclic voltammograms of MB in the absence and presence of (A) EAD2 and (B) RDNA.

Table S4 shows that both anodic and cathodic peak potentials of MB in the presence of EAD2 and RDNA shift to a more negative value compared with a solution of free MB without DNA. ΔE_p, the separation of the cathodic and anodic peak potentials, is in the range of 70 - 85 mV, indicating a quasi-reversible single electron redox process. $E_{1/2}$, the average of cathodic and anodic peak potentials, shift from -0.242 V to -0.278 V for EAD2, while from -0.245 V to -0.262 V for RDNA. The net shift of $E_{1/2}$ can be used to estimate the ratio of the equilibrium constants for the binding of MB (oxidized form) and MBH (reduced form) to DNA.[32]

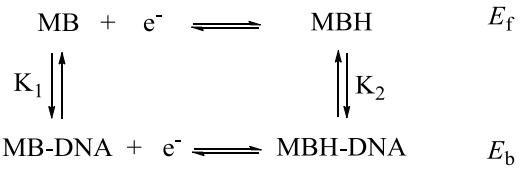

Scheme 1. The illustration of MB binding to DNA in different forms.

In scheme 1, E_f and E_b are the formal potentials of MB/MBH in free and bound forms, respectively, while K_1 and K_2 are the corresponding binding constants for MB and MBH to DNA. For this redox process, the relation between E_f and E_b can be expressed as:

$$E_b - E_f = 0.059 \log(K_2/K_1)$$

Thus, for limited shifts of -36 mV and -17 mV for MB when binding with EAD2 and RDNA, respectively, K_1/K_2 were calculated as 4.07 and 1.94. That is to say, the DNA binding ability for MB in its oxidized form was stronger than in its reduced form, even when MB bound with the random DNA sequence. This difference might be due to the different electrostatic attraction between negatively charged DNA backbone and positively charged MB in different forms. The oxidized form of MB with one more proton is more positive compared with the reduced form. The lower diffusion current at the same molar ratio R value means that MB is more favored and specific in binding with G-quadruplex.

Thermodynamic analysis by ITC

ITC experiments were conducted to extract thermodynamic parameters for the MB binding event with different intramolecular G-quadruplexes with different conformations under the same conditions. A parallel type (EAD2), coexisting or mixed hybrid type (HT) and antiparallel G-quadruplex (TA) were involved.

First, MB dilution was studied and we observed an exothermic process with non-constant heats of dilution (Figure 5A), which suggested stepwise self-aggregation.[33, 34] Data fitting using ITC-ITC[35, 36] gave an equilibrium constant K_{agg} of 1.4×10^3 M^{-1} and an enthalpy change for aggregation ΔH_{agg} of -15.8 kcal·mol^{-1} for this process (as shown in Figure 5B; fittings and evaluation of error margins for the parameters were recorded in Figure S6). In the binding titrations, MB was injected stepwise into solutions of G-quadruplexes with different conformations and the resulting enthalpograms are shown in Figure 6.

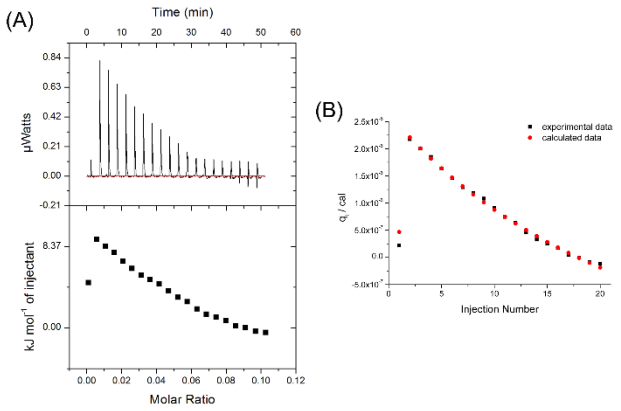

Figure 5. (A) Heat effects for the dilution of 500 μM MB at 25℃; (B) The fitting of stepwise self-aggregation of MB.

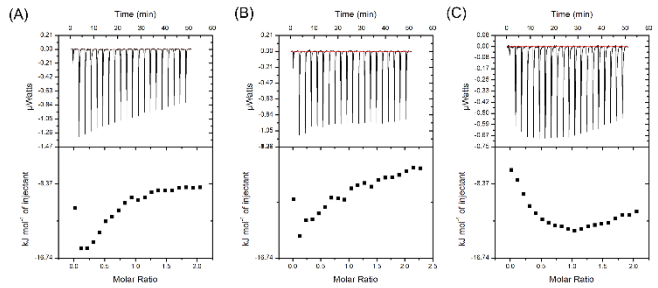

Figure 6. Enthalpograms for the binding of MB with (A) parallel G-quadruplex EAD2, (B) coexisting or mixed hybrid type HT and (C) antiparallel G-quadruplex TA.

From Figure 6, we observe that the binding of MB with different intramolecular G-quadruplexes with different conformations changes from one binding site (Figure 6A and 6B) to two binding sites (Figure 6C). Comparison of binding data with the dilution data further shows that binding of MB with quadruplex structures is exothermic. Evaluating the ITC data (see SI), MB bound with parallel G-quadruplex sequence EAD2 stronger (K_{A1} = 2.7×10^4 M^{-1}) than with the coexisting or mixed hybrid type HT (K_{A1}= 2000-6000 M^{-1}). Compared with binding to parallel G-quadruplex sequence EAD2, the binding of MB to coexisting or mixed hybrid type HT is too weak to allow to exactly quantify the binding parameters via IC-ITC software (Figure S7-S10). However, in the situation of antiparallel G-quadruplex TA, the binding model suggested two types of binding sites (Figure S11–S12). In all cases, the binding strength is weaker than that caused by some large aromatic molecules, such as the tetraazaperopyrene molecule, which has extended flat aromatic structure and can bind with the parallel G-quadruplex conformation of c-myc via end-stacking.[34] These ITC data supports the electrochemical results well and suggest that MB interacts with intramolecular G-quadruplexes is not similar with large π surface molecules.

Conclusions

In summary, we investigated the interaction between MB and different intramolecular G-quadruplexes by electrochemistry, and validated our studies using CD, molecular docking and ITC. From the results of the experiments, MB might interact with intramolecular G-quadruplexes with stacking up to two guanine bases, which is different from other large π-aromatic molecules stacking with four guanines. And the binding model in antiparallel intramolecular G-quadruplex also contains the non-negligible non-specific electrostatic or other interactions. Importantly, the study of the HT sequence under varying ionic conditions shows that interaction strength is dependent on the conformation of quadruplexes and this dependence can be easily and fast obtained by electrochemical technique, which can also give an explicit binding affinity discrimination. The electrochemical approach is a good tool for the interaction study between MB and G-quadruplexes and shows potential for the investigation on the conformation change of G-quadruplex under different conditions. What's more, it also provides a new strategy to study the ligands of G-quadruplexes and ligands and is useful for the G-quadruplex ligand screening.

Acknowledgements

This work was supported by the National Natural Science Foundation of China (No. 21675004, 21575005 and 21275009). We thank for the JASCO CD spectrometer to Prof. G. Yuan and also give our acknowledgement for MicroCal iTC 200 equipment to Prof. L. H. Lai.

Notes and references

1. M. Gellert, M. N. Lipsett and D. R. Davies, *Proc. Natl. Acad. Sci. U. S. A.*, 1962, **48**, 2013-2018.
2. G. N. Parkinson in Quadruplex nucleic acids (Eds.: S. Neidle, S. Balasubramanian), Vol. 7, Royal Society of Chemistry, 2006, pp. 1-30.
3. A. Randazzo, G. P. Spada, and M. W. D. Silva in Topics in current Chemistry (Eds.: J. B. Chaires, D. Graves), Vol. 330, Springer, 2013, pp. 67-86.
4. V. T. Mukundan and A. T. Phan, *J. Am. Chem. Soc.*, 2013, **135**, 5017-5028.
5. J. E. Johnson, J. S. Smith, M. L. Kozak and F. B. Johnson, *Biochimie*, 2008, **90**, 1250-1263.
6. Y. Qin and L. H. Hurley, *Biochimie*, 2008, **90**, 1149-1171.
7. E. Henderson, C. C. Hardin, S. K. Walk, I. Tinoco and E. H. Blackburn, *Cell*, 1987, **51**, 899-908.
8. V. S. Chambers, G. Marsico, J. M. Boutell, M. Di Antonio, G. P. Smith and S. Balasubramanian, *Nat. Biotechnol.*, 2015, **33**, 877-881.
9. H. Han and L. H. Hurley, *Trends Pharmacol. Sci.*, 2000, **21**, 136-142.
10. Y. Jiang, A. C. Chen, G. T. Kuang, S. K. Wang, T. M. Ou, J. H. Tan, D. Li and Z. S. Huang, *Eur. J. Med. Chem.*, 2016, **122**, 264-279.
11. D. Drygin, A. Siddiqui-Jain, S. O'Brien, M. Schwaebe, A. Lin, J. Bliesath, C. B. Ho, C. Proffitt, K. Trent, J. P. Whitten, J. K. Lim, D. Von Hoff, K. Anderes and W. G. Rice, *Cancer Res.*, 2009, **69**, 7653-7661.
12. E. Golub, R. Freeman and I. Willner, *Anal. Chem.*, 2013, **85**, 12126-12133.
13. F. T. Zhang, J. Nie, D. W. Zhang, J. T. Chen, Y. L. Zhou and X. X. Zhang, *Anal. Chem.*, 2014, **86**, 9489-9495.
14. A. Laguerre, K. Hukezalie, P. Winckler, F. Katranji, G. Chanteloup, M. Pirrotta, J.-M. Perrier-Cornet, J. M. Y. Wong and D. Monchaud, *J. Am. Chem. Soc.* , 2015, **137**, 8521-8525.
15. A. De Rache, T. Doneux and C. Buess-Herman, *Anal. Chem.*, 2014, **86**, 8057-8065.
16. Q. Fan, C. Li, Y. Tao, X. Mao and G. Li, *Talanta*, 2016, **160**, 144-147.
17. Y. Jin, X. Yao, Q. Liu and J. Li, *Biosens. Bioelectron.*, 2007, **22**, 1126-1130.
18. M. Ortiza, A. Fragosoa, P. J. Ortizb and C. K. O'Sullivan, *J. Photoch. Photobio. A*, 2011, **218**, 26-32.
19. N. H. Campbell, G. N. Parkinson, A. P. Reszka and S. Neidle, *J. Am. Chem. Soc.*, 2008, **130**, 6722-6724.
20. L. Ginnari-Satriani, V. Casagrande, A. Bianco, G. Ortaggi and M. Franceschin, *Org. Biomol. Chem.*, 2009, **7**, 2513-2516.
21. G. N. Parkinson, R. Ghosh and S. Neidle, *Biochemistry*, 2007, **46**, 2390-2397.

22. D. S. Chan, H. Yang, M. H. Kwan, Z. Cheng, P. Lee, L. P. Bai, Z. H. Jiang, C. Y. Wong, W. F. Fong, C. H. Leung and D. L. Ma, *Biochimie*, 2011, **93**, 1055-1064.
23. H. Sun, J. Xiang, Y. Zhang, G. Xu, L. Xu and Y. Tang, *Chinese Sci. Bull.*, 2006, **51**, 1687-1692.
24. X. Cheng, X. Liu, T. Bing, Z. Cao and D. Shangguan, *Biochemistry*, 2009, **48**, 7817-7823.
25. D. W. Zhang, J. X. Liu, J. Nie, Y. L. Zhou and X. X. Zhang, *Anal. Chem.*, 2013, **85**, 2032-2036.
26. O. Trott and A. J. Olson, *J. Comput. Chem.*, 2010, **31**, 455-461.
27. G. N. Parkinson, M. P. Lee and S. Neidle, *Nature*, 2002, **417**, 876-880.
28. A. Matsugami, Y. Xu, Y. Noguchi, H. Sugiyama and M. Katahira, *The FEBS journal*, 2007, **274**, 3545-3556.
29. Y. Wang and D. J. Patel, *Structure*, 1993, **1**, 263-282.
30. E. F. Pettersen, T. D. Goddard, C. C. Huang, G. S. Couch, D. M. Greenblatt, E. C. Meng and T. E. Ferrin, *J. Comput. Chem.*, 2004, **25**, 1605-1612.
31. Available upon request from Niklaas J. Buurma.
32. M. T. Carter, M. Rodriguez and A. J. Bard, *J. Am. Chem. Soc.* , 1989, **111**, 8901-8911.
33. E. H. Braswell, *J. Phys. Chem.*, 1984, **88**, 3653-3658.
34. L. Hahn, N. J. Buurma and L. H. Gade, *Chemistry*, 2016, **22**, 6314-6322.
35. N. J. Buurma and I. Haq, *Methods*, 2007, **42**, 162-172.
36. N. J. Buurma and I. Haq, *J. Mol. Biol.*, 2008, **381**, 607-621.